Parametric Analysis of Thermal Swing Cycles for Multicomponent Adsorption

A study was made of the effect of design and operating parameters on the regeneration of a fixed bed of activated carbon. Two adsorbed species were removed by a hot gas purge, making the study relevant to thermal swing cycles used commercially. The analysis utilized direct experimental results as well as simulated results using a model described earlier by the authors (Huang and Fair, 1988).

Regeneration parameters studied were: type of purge gas, purge gas contact time and velocity, regeneration temperature, initial bed loading, and bed pressure. These were related to certain parameters influencing the adsorption step: type of carrier gas, feed concentration, contact time and velocity, pressure, and initial bed temperature. The results are summarized in the form of guidelines for optimal regeneration cycle specification.

Chen-Chia Huang
James R. Fair
Department of Chemical Engineering
University of Texas
Austin, TX 78712

A thermal swing adsorption (TSA) cyclic process includes both adsorption and thermal purge steps. Despite its energy intensiveness, the purge step has received very little attention in the past, particularly for the nonequilibrium condition that exists in all commercial adsorption systems. On the other hand, the adsorption step has received widespread attention when single-component adsorption is involved, but relatively little attention when multiple adsorbates are involved.

Basmadjian et al. (1975a) were the first workers to provide a model for thermal purge regeneration, but their model did not take into account heat or mass transfer limitations and assumed equilibrium at all times during the purge cycle. Their model was limited also to a single adsorbate. Kumar and Dissinger (1986) proposed a nonequilibrium purge model based on the data of Basmadjian et al. Recently Schork and Fair (1988) developed a new nonequilibrium model using variable, lumped-resistance mass transfer coefficients, and studied the effect of several operating parameters on the regeneration efficiency of a bed of activated carbon. This earlier work, however, did not account for more than one solute being present for adsorption and regeneration. Accordingly, the authors extended the work to the multicomponent adsorption/desorption case (Huang and Fair, 1988).

The purpose of the present paper is to provide a parametric analysis of thermal swing adsorption when two adsorbates are involved and thus to provide a rational study of the variables that, when properly manipulated, can lead to significant reductions in energy consumption, at least compared with empirical approaches that have been used in the past. The parameters studied include the nature of carrier gas, feed concentration, feed rate, initial bed temperature, operating pressure, initial bed loading, and regeneration temperature.

Experimental Work

Ethane, propane, and their mixtures were adsorbed onto and desorbed from Witco JXC activated carbon. Properties of the carbon adsorbent are shown in Table 1. Helium and nitrogen were used as carrier gases during adsorption and as purge gases during regeneration. Analyses were made by gas chromatography, using flame ionization detectors. The adsorption bed was oriented vertically and was 30.5-cm long and 7.44-cm inside-diameter. Several thermocouples were connected to a digital thermometer through a relay system controlled by a computer. The data acquisition system allowed all thermocouples to be read within 5 seconds, and temperatures were recorded every 15 s. For a detailed description of the experimental system, the reader may refer to Huang and Fair (1988).

Mathematical Modeling

A dynamic model, representing the mass and energy balances for fixed-bed adsorption and desorption, as well as a numerical approach, has been described in detail in the earlier paper (Huang and Fair, 1988). For a gas adsorption process with two adsorbates, there are seven partial differential equations repre-

The current address of C-C Huang is Department of Applied Chemistry, Chung Cheng Institute of Technology, Tashi, Taoyuan, Republic of China (Taiwan).

Table 1. Physical Properties of Witco JXC Activated Carbon

	Manufacturer's Data	Experimental Data		
US Mesh Size		4 × 6	6 × 8	8 × 10
Surface Area (m^2/kg)	1.10×10^6	1.14×10^6	1.26×10^6	1.16×10^6
Bulk Density (kg/m^3 bed)	4.81×10^3 (Max)	4.63×10^3	4.65×10^3	4.61×10^3
Specific Heat ($J/kg \cdot K$)	8.37×10^2 (367K) 1.17×10^3 (700K)	—	—	—
Geometric Surface Area a_p (m^{-1})		1.32×10^3	1.97×10^3	2.41×10^3
Porosity ϵ_p		0.59	0.58	0.60
Bed Void Fraction ϵ_{ex}		0.44	0.45	0.44

senting energy and mass balances within the packed bed. The mass flux into the solid particles is represented by a linear driving force model with variable lumped-resistance transfer coefficients. The Flory-Huggins form of the Vacancy Solution Model (Cochran et al., 1985) was employed to calculate the interfacial equilibrium concentration.

Parametric Analysis

The adsorption and regeneration cycle runs made for the present study are described in Table 2. Run numbers for adsorption and regeneration correspond to each other. The gas flow rates used span the range of typical industrial operations. The propane and/or ethane concentration in the feed gas stream for adsorption ranged from 0.0 to 1.5 mol %. The direction of gas flow for regeneration was countercurrent to that for adsorption. It was found that the flow direction had no significant effect on breakthrough curves for this test system. The bed was taken to full saturation in all adsorption runs except for AD-21, which was halted at propane breakthrough. For a particular complete cycle, the carrier gas and the purge gas were the same, whether helium or nitrogen.

A combination of experimental results and computer simulations was used to study the effect of various operating parameters on the breakthrough and depletion curves. Operating conditions for AD/DE-22 were taken as the base for computer simulations; variations from these conditions are noted in the discussion.

Adsorption Step

Carrier gas

Nitrogen may compete with ethane for adsorption on carbon when the partial pressure of nitrogen is much higher than that of ethane (Huang and Fair, 1988). Experimental confirmation of this is illustrated in Figure 1. The operating conditions for the two runs were the same, except for the carrier gas used. The ear-

Table 2. Operating Conditions of Adsorption Runs

Run No.	Adsorption step						Regeneration step			
	y_c3in	y_c2in	$G \times 10^{+3}$		T_{inlet}	P	$G \times 10^{+3}$		T_{reg}	P
	mol %		kmol/m²·s	Inert	K	kPa	kmol/m²·s	Purge	kmol/m²·s	kPa
3*	0.74	0.75	5.21	N_2	294.9	170	5.14	N_2	344.1	170
4*	0.73	0.77	6.95	N_2	293.3	170	6.85	N_2	353.4	170
5*	0.74	1.48	7.19	N_2	295.4	170	7.00	N_2	360.6	170
6	0.71	0.75	5.21	He	295.3	170	5.14	He	352.2	170
7	1.48	0.72	5.26	N_2	295.9	170	5.14	N_2	369.4	170
8	1.50	0.72	5.28	He	295.6	170	5.16	He	360.4	170
9	1.50	0.72	5.26	He	295.1	170	5.10	N_2	363.6	170
10	1.47	1.48	3.53	N_2	295.4	170	3.41	N_2	362.1	170
11	1.52	1.52	5.31	N_2	295.6	170	5.10	N_2	374.9	170
12	0.75	0.73	5.17	N_2	295.1	239	5.04	N_2	380.4	239
13	1.51	1.53	5.48	He	295.1	170	5.28	He	369.3	170
14	0.70	0.73	5.21	He	295.2	239	5.14	He	368.2	239
15	0.72	1.38	7.32	He	296.0	170	5.14	He	352.5	170
17	0.0	0.73	5.17	N2	295.8	239	5.12	N_2	375.4	239
21**	0.71	0.75	5.21	N2	296.4	239	5.14	N_2	376.0	239
22*	0.71	0.73	5.21	N2	294.8	239	5.14	N_2	375.4	239
24	0.0	0.76	5.20	He	292.4	239	5.16	He	372.1	239
25	0.74	0.0	5.16	N2	294.4	239	5.10	N_2	372.1	239
26	0.70	0.0	5.20	He	296.1	239	5.16	He	372.1	239

*Downward run for adsorption step
**Partial saturation run
Note: In the text and in figures adsorption runs carry the prefix AD, and the corresponding regeneration runs carry the prefix DE.

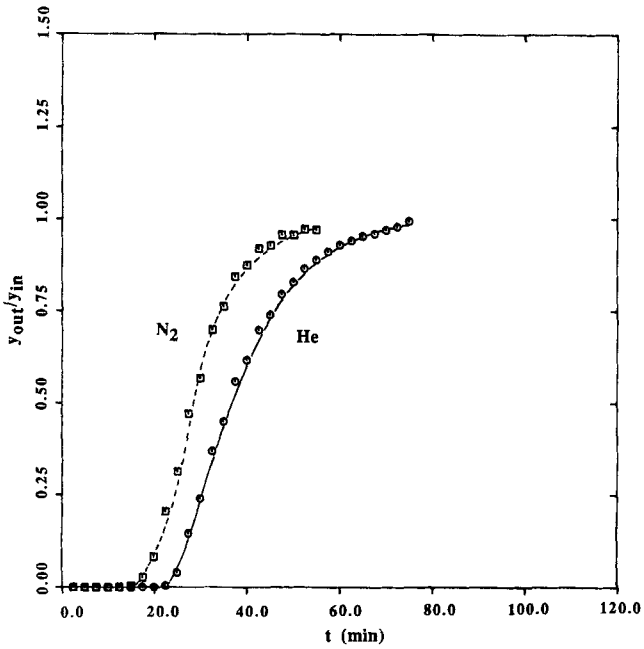

Figure 1. Effect of carrier gas on ethane breakthrough for single-solute adsorption.
Runs AD-17 (N_2) and AD-24 (He)

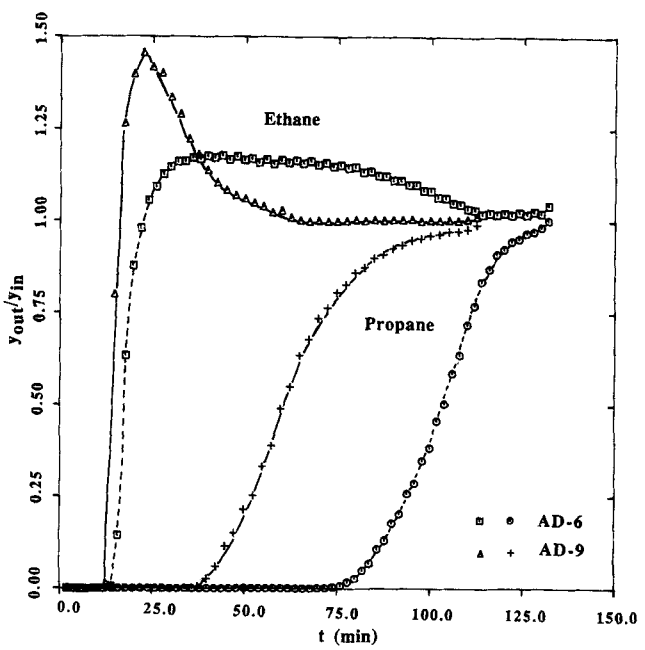

Figure 3. Effect of propane inlet concentration on breakthrough.
Runs AD-6 (y_{c3in} = 0.71%) and AD-9 (y_{c3in} = 1.50%)

lier breakthrough using nitrogen as the carrier indicates some nitrogen sorption, since helium is known not to be adsorbed. For propane adsorption, the carrier gas effect is not so significant, since propane is much more strongly adsorbed than nitrogen.

Feed concentration

Figures 2 and 3 illustrate the effect of inlet concentrations of ethane and propane, respectively. For Run AD-11, the ethane concentration was about double that of Run AD-7. The remaining operating conditions for these two runs were essentially identical. For Run AD-9, the propane concentration was almost double that of Run AD-6, with other conditions unchanged. It is clear that, the higher the inlet concentration, the earlier the breakthrough for the same total flow rate. A comparison of Figures 2 and 3 reveals that the effect of inlet concentration is much more significant for propane than for ethane. This is because propane is more strongly adsorbed on activated carbon than ethane; the isotherm of propane is steeper and more favorable. For a favorable isotherm system, the loading capacity of adsorbent increases along with the gas-phase concentration. The increase is not linear, however. The loading capacity increment, due to doubling the propane inlet concentration, was trivial compared to its total loading capacity. Therefore, the breakthrough time for doubled propane inlet concentration was about half of its original breakthrough time. For ethane runs, however, the increment of loading capacity was significant compared to its original capacity, and there was little change in breakthrough time.

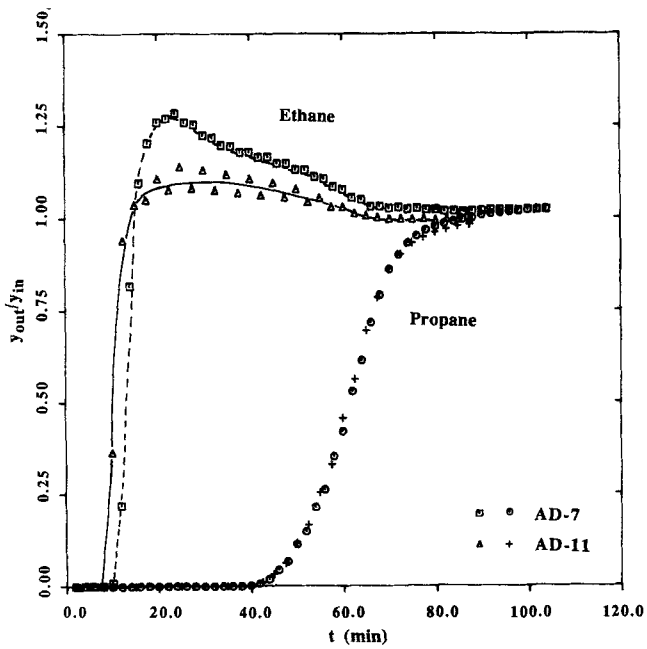

Figure 2. Effect of ethane inlet concentration on breakthrough.
Runs AD-7 (y_{c2in} = 0.72%) and AD-11 (y_{c2in} = 1.52%)

It is worth noting that a change of inlet concentration of the nonkey component (ethane) has little effect on the breakthrough of the key component, but this is not true in reverse. As Figure 3 shows, the higher the propane inlet concentration, the higher the ethane "roll-up" and the earlier the ethane breakthrough.

Figure 4 represents the effect of inlet composition on the breakthrough curves, based on computer simulations. Curve 1 represents the case of a single adsorbate, either ethane or propane. The remaining curves are the bisolute cases with different inlet concentrations. For single-component adsorption, the breakthrough curve is generally sigmoid. For multicomponent adsorption, however, the nonkey component breakthrough curve always overshoots its inlet concentration. The height of roll-up

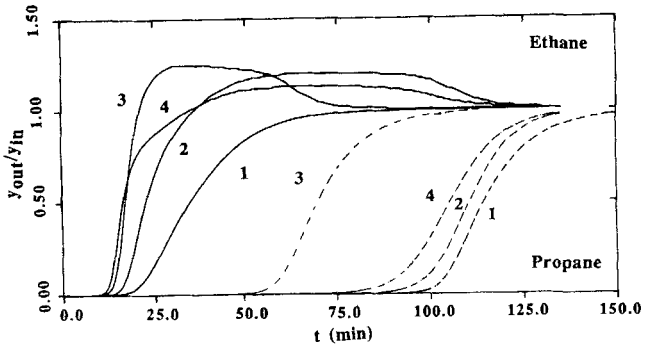

Figure 4. Effect of inlet composition on breakthrough (based on simulations).

1. single adsorbate $y_{c2in} = 0.73\%$ or $y_{c3in} = 0.71\%$
2. $y_{c2in} = 0.73\%$, $y_{c3in} = 0.71\%$
3. $y_{c2in} = 0.73\%$, $y_{c3in} = 1.50\%$
4. $y_{c2in} = 1.50\%$, $y_{c3in} = 0.71\%$

(——, ethane; ------, propane)

of the nonkey component varies with the inlet compositions of both nonkey and key components. The overshoot increases with decreasing ethane concentration at constant propane feed level. This is the result of relative competition between adsorbates. The nonkey component adsorbability is decreased with decreasing concentration at the same temperature, since that component at a downstream location is more readily displaced by the key component. On the other hand, the height of roll-up increases with increasing propane concentration, at a constant ethane feed level. The key component has a greater competitive capability at a higher concentration. Consequently, more of the nonkey component is displaced downstream.

The shape of the breakthrough curve of the key component remains the same for both single-component and multicomponent adsorption processes, and is little affected by the nonkey component. The effect of varying nonkey component feed concentration on the complete breakthrough time of the key component is small. Varying the key component feed concentration has a much more significant effect on its breakthrough curve, since the higher the concentration, the sooner it elutes. Gariepy and Zwiebel (1971) and Madey et al. (1986) have reported similar findings with regard to inlet composition effects.

Contact time and velocity

The effect of flow rate on breakthrough curves is illustrated in Figure 5. Since higher flow rates bring more adsorbates into the bed per unit time, breakthroughs are expected to be earlier. The time difference between propane breakthrough and ethane breakthrough increases for the low flow rate run. Accordingly, for a given height of bed, the adsorptive separation will improve at a lower superficial velocity.

As shown in Table 2, Runs AD-4 and AD-10 were operated under the same conditions, except that the flow rate of AD-4 was double that of AD-10. To compensate for this, the ethane and propane concentrations for AD-4 were only half of those for AD-10. Thus, the same amounts of adsorbates were fed into the bed per unit time for the two runs. The breakthrough curves for the runs are presented in Figure 6. It may be observed that both adsorbates appeared a little earlier in Run AD-4 than they did in Run AD-10; flow rate appears to have a more significant effect than inlet concentration on the adsorption process.

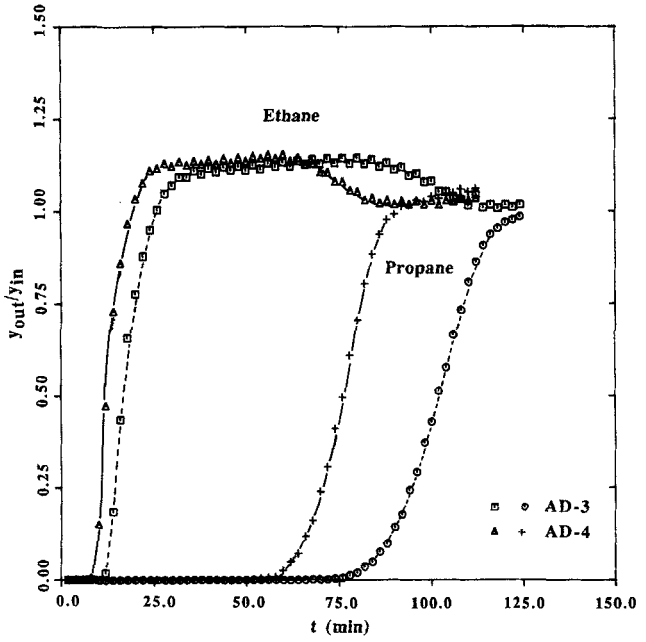

Figure 5. Effect of flow rate on breakthrough.

Runs AD-3 ($G = 5.21 \times 10^{-3}$ kmol/m^2 · s)
AD-4 ($G = 6.95 \times 10^{-3}$ kmol/m^2 · s)

For a bed of given height, varying the gas velocity will vary the contact time. In order to analyze the effect of velocity alone, the contact time must be maintained constant as the gas flow rate is varied, which requires varying bed height. The effect of superficial velocity on the breakthrough curves, at constant contact time, is shown in Figure 7. The difference between the curves is only slight; this is to be expected since the primary

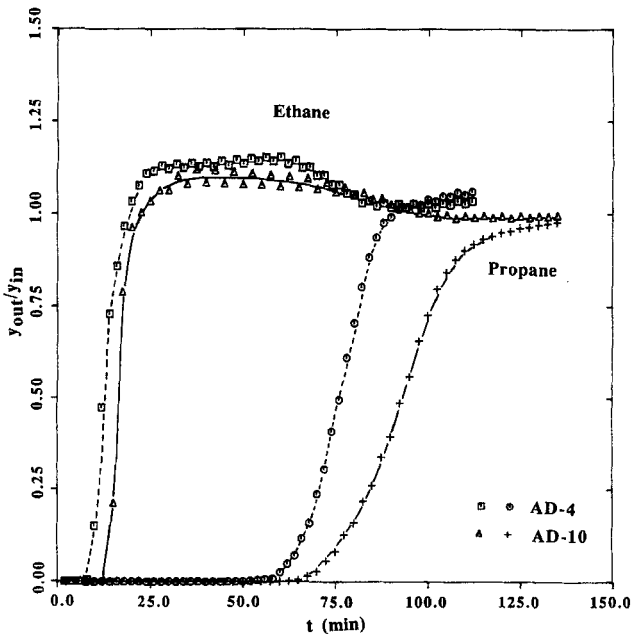

Figure 6. Effect of inlet concentration and flow rate on breakthrough.

Runs AD-4 ($y_{c2in} = 0.77\%$, $y_{c3in} = 0.73\%$, $G = 6.95 \times 10^{-3}$ kmol/m^2 · s) AD-10 ($y_{c2in} = 1.46\%$, $y_{c3in} = 1.47\%$, $G = 3.53 \times 10^{-3}$ kmol/m^2 · s)

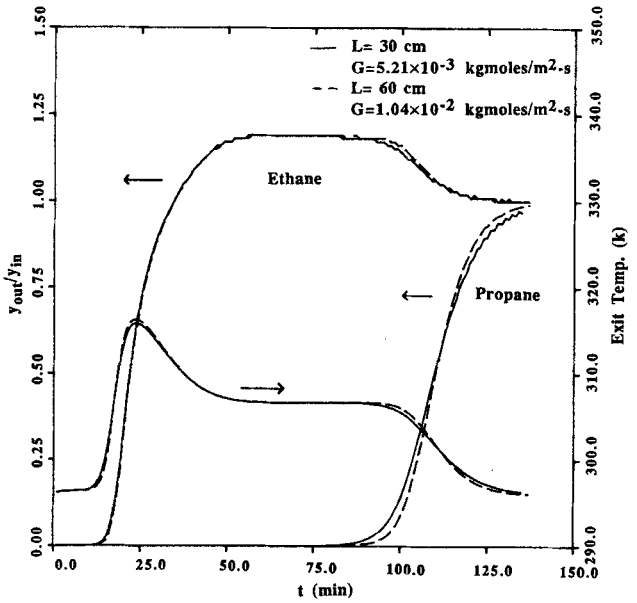

Figure 7. Effect of gas velocity on breakthrough at constant contact time (based on simulation): adiabatic case.

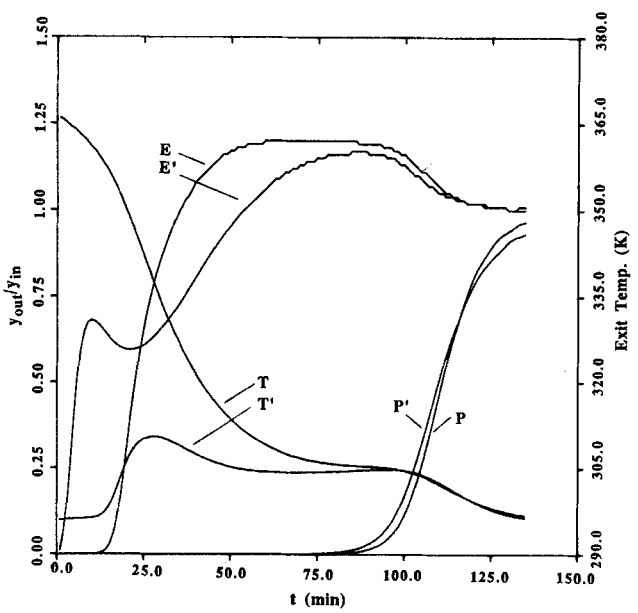

Figure 8. Effect of initial bed temperature on breakthrough (based on simulation).
$T_{bed,i}$ = 296 K (P, E, T)
$T_{bed,i}$ = 367 K (P^1, E^1, T^1)

resistance to mass transfer is intraparticle, while only the film resistance is affected by gas velocity. The breakthrough curve of propane from the longer bed is seen to be slightly sharper, because of increased mass and heat transfer rates at the higher gas velocity.

Initial bed temperature

If the following criteria are met, the cooling step after thermal regeneration may be omitted (Basmadjian, 1975):

$$\frac{W_F}{y_F} > \frac{c_{ps}}{c_{pg}} \tag{1}$$

and

$$\frac{W_p}{y_F} > \frac{3}{2}\frac{c_{ps}}{c_{pg}} \tag{2}$$

The plateau temperature, T_p, is obtained from:

$$T_p = T_F - \frac{W_F \Delta H}{c_{pg}(W_F/y_f) - c_{ps}} \tag{3}$$

In the present study, all cases satisfy the first criterion, Eq. 1. The propane adsorbate in either nitrogen or helium meets the second criterion, Eq. 2, but the ethane adsorbate does not.

The effect of initial bed temperature on the breakthrough curves is illustrated in Figure 8. Curves P, E, and T represent the base case with an initially cold bed. Curves P^1, E^1, and T^1 represent the case of an initially hot bed. There is little effect on the propane breakthrough curve, as expected. The temperature decreases since the feed stream is cold and offsets the heat of adsorption. Conversely, the ethane breaks through the hot bed very quickly. The effluent ethane concentration has a dip, since the ethane is readsorbed downstream as the bed temperature decreases to a certain value. Because of the displacement by propane, the ethane breakthrough curve increases again and overshoots its feed concentration.

For separation purposes, the initial hot bed worked well in the present study. It would appear that despite a lower separation efficiency for the hot bed, in a practical way the cooling step may be omitted in the thermal swing cyclic process. More detailed discussion on this point is presented later. The Basmadjian criteria (Eqs. 1 and 2) appear to apply equally well for multicomponent adsorbates.

Bed pressure

The effect of total bed pressure is presented in Figure 9. From isotherm data, it is clear that the bed loading capacity increases when the partial pressures of the adsorbates increase. Thus, the breakthrough times increase with increasing pressure. Since propane is more strongly adsorbed, the pressure effect on its breakthrough is more significant. The ethane-propane separation is favored by higher system pressures.

Regeneration Step

Before discussing parametric studies of regeneration, the following should be noted. First, all the experimental regeneration runs were continued from previous adsorption runs in order to complete the cycle. Therefore, initial bed conditions for different runs, except for the parameter to be studied, might not be the same. Secondly, the heaters for the purge gas were manually controlled, and it is difficult to obtain the exact same inlet temperature of purge gas for different runs. An effort was made, however, to reach the same desired conditions insofar as was possible.

Three parameters are of importance in the discussion of regeneration of a fixed-bed adsorber: the quantity of regenerant required, the total energy required, and the total regeneration

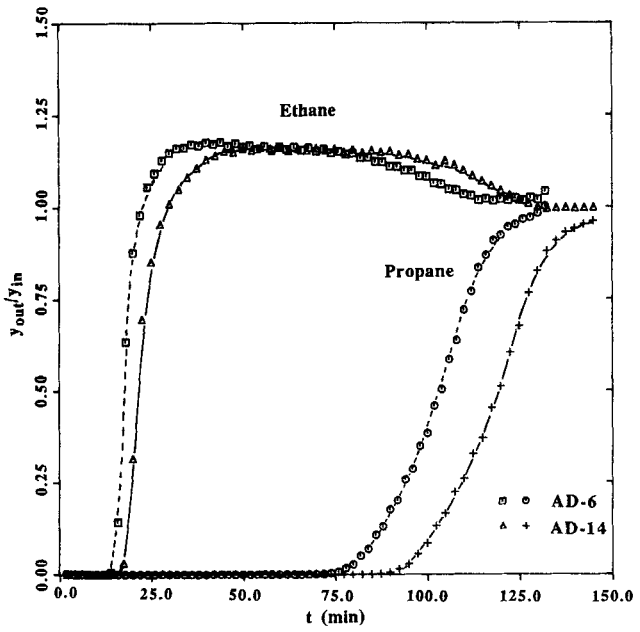

Figure 9. Effect of pressure on breakthrough.
Runs AD-6 (P = 170 kPa) and AD-14 (P = 239 kPa).

time. The first two parameters are generally discussed in terms of quantity of purge per kilogram of adsorbent, n, and energy per kilogram of adsorbent, Q, to represent regeneration efficiency. The third parameter is important in the design of a cyclic adsorption process. The ratio of regeneration time to adsorption time determines the number of beds required to maintain continuous operation.

Owing to the displacement of ethane by propane during the adsorption step, only a small amount of ethane (nonkey component) remains in the bed after propane breakthrough. Most of the ethane is purged out quickly. Therefore, for a discussion of regeneration of a multisolute adsorber, the depletion curve of the key component (propane) should be emphasized. Since the effluent concentration approaches zero asymptotically, the conditions at which regeneration is considered complete must be defined. Kumar and Dissinger (1986) defined regeneration to be complete when the effluent gas reaches the regeneration temperature for an adiabatic system. The definition of Schork (1986) defines regeneration as occurring when the effluent concentration reaches 1.0% of the corresponding adsorption feed concentration. This "complete" time is designated as $t_{1\%}$. The Schork definition is good for both adiabatic and nonadiabatic systems, and was employed in this study; the regeneration time $t_{1\%}$ is related to the key component of the multisolute system. The required amounts of regenerant and specific energy are calculated from the following equations,

$$n = \frac{Gt_{1\%}}{L\rho_b} \tag{4}$$

$$Q = nc_{pg}(T_{reg} - T_o) \tag{5}$$

a reference temperature of 294 K is used.

The depletion curve of the key component in a regeneration multisolute adsorber is a typical two-zone type. The two mass transfer zones are separated by a concentration plateau. Because of the spreading of the transfer zones, the plateau might be eliminated and form a peak. The shapes of the depletion curves of the key component will be discussed in terms of the height of the concentration plateau or peak and the width of the mass transfer zones.

Purge gas

Helium and nitrogen were used as purge gases for regeneration runs. For a single adsorbate system, as Figure 10 shows, the hot nitrogen served as a much better regenerant than did the hot helium. The height of the "roll-up" peak for nitrogen purge was much higher than that for helium purge; this is because of the higher heat capacity of nitrogen. The high heat capacity purge gas brings much more energy into the bed under the same volume flow rate, and the bed temperature increases much faster. This was verified by heating a clean bed by hot nitrogen and by hot helium (Huang, 1987). For higher bed temperatures, the adsorbate diffuses out of the adsorbent much faster. It should be noted in Figure 10 that the effluent concentration of ethane did not overshoot the corresponding inlet concentration, for the hot helium purge run, even though the inlet temperature of the purge gas was higher than 372 K.

For multicomponent adsorption runs, only a fraction of the nonkey component is left in the bed after complete breakthrough of the key component. Thus, the depletion curve of the nonkey component drops very fast, no matter what kind of regenerant is used. This is clearly illustrated by the ethane depletion curves in Figure 11. However, depletion curves of the key component for a multisolute system are similar to those for a single component system. The effect of purge gas is also the same as discussed for the single-solute case.

The depletion curves for different purge gases (nitrogen and helium) regenerating a completely adiabatic bed are studied theoretically with the operating conditions of Run DE-22. The

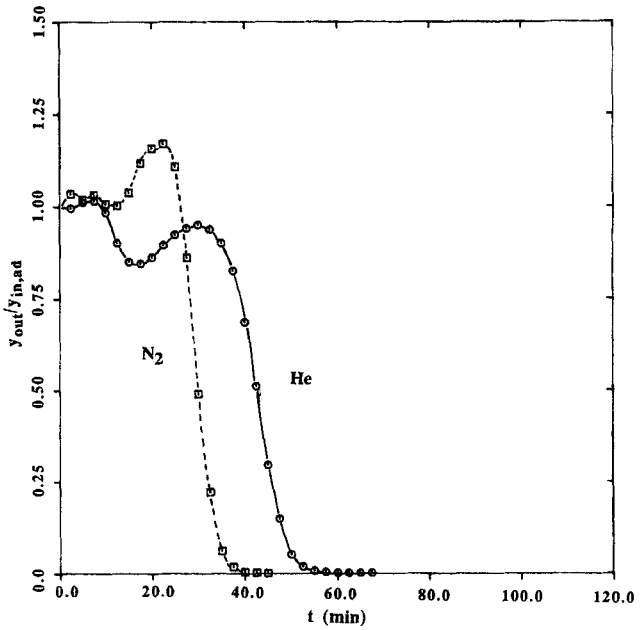

Figure 10. Effect of purge gas on ethane depletion for single-solute desorption.
Runs DE-17 (N_2) and DE-24 (He)

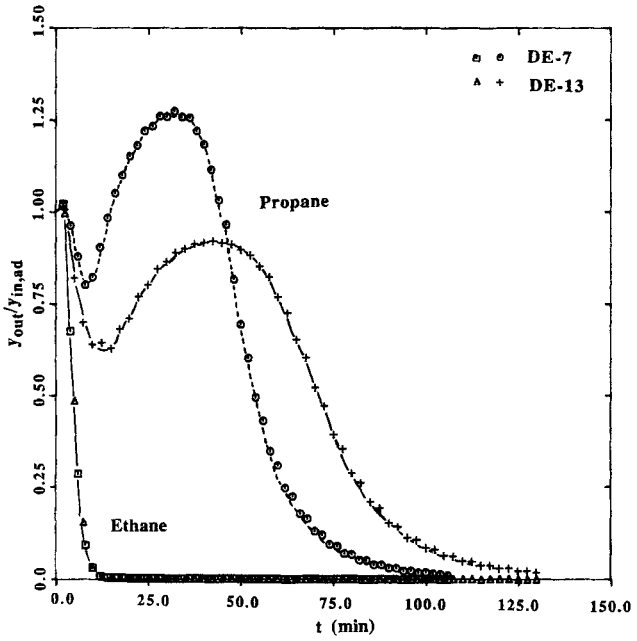

Figure 11. Effect of purge gas on depletion curves for bisolutes desorption.
Runs De-7 (N_2) and DE-13 (He)

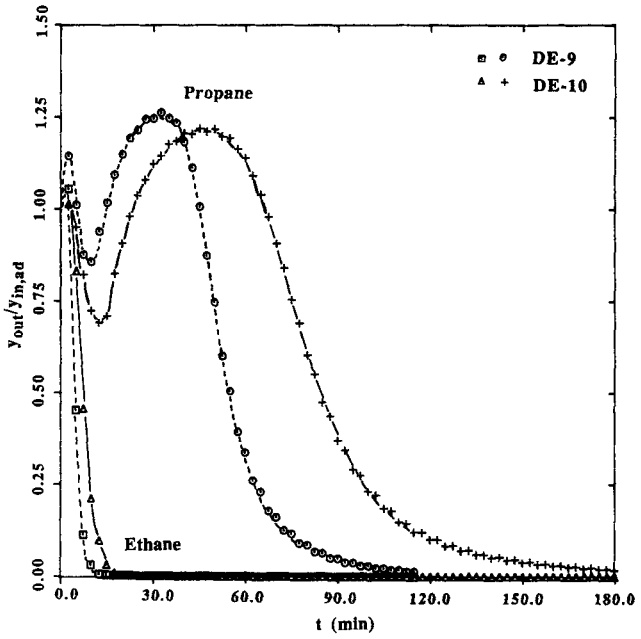

Figure 12. Effect of flow rate on depletion curves.
Runs DE-9 ($G = 5.10 \times 10^{-3}$ kmol/m^2 · s)
DE-10 ($G = 3.41 \times 10^{-3}$ kmol/m^2 · s)

total regeneration time for nitrogen purge is about 13 minutes, less than that for the helium purge. The purge gas requirements are 0.147 and 0.173 kg mol/kg adsorbent for nitrogen and helium purge, respectively. The specific energy requirements for nitrogen and helium runs are 344.2 and 285.2 kJ/kg of carbon, respectively. The height of roll-up is higher for nitrogen than for helium purge. The heat capacities of nitrogen and helium at the regeneration temperature are 29.56 and 20.72 kJ/kg · K, respectively. Therefore, it can be concluded that the higher heat capacity regenerant (nitrogen) has an advantage of high roll-up value, low specific purge gas requirement, and less total regeneration time, while the heat load remains nearly constant. A similar conclusion was drawn by Basmadjian et al. (1975a) for single-component desorption.

Contact time and velocity

The effect of varying the purge gas flow rate with constant height of bed is illustrated in Figure 12. It is clear that increasing the purge rate shifts the peak position of the key component depletion curve to the left and decreases the regeneration time. The peak height changed very little when the purge gas flow rate was changed. However, the dip of the propane depletion curve was more prominent for the lower purge gas flow rate. This is because the bed is heated up slowly for the lower purge rate, and the initial desorption rate is too low.

The effect of superficial velocity at constant contact time on the depletion curves is presented in Figure 13. The curves are based on simulation results for a completely adiabatic bed. The contact times of the two runs are the same. As for adsorption, the difference in the depletion curves is insignificant, because the primary resistance to mass transfer is intraparticle, which is unaffected by the superficial velocity of the purge gas.

The effect of contact time can be studied by observing the propagation of a concentration front moving through a bed. Figure 14 shows a propane concentration front traveling through a 60-cm-long adiabatic bed. A fully-developed depletion curve comprises two transfer zones, separated by a concentration plateau. With very short contact time, however, the transfer zones may overlap and the plateau is lost. As shown in Figure 14, the concentration profile is not fully developed in a 15-cm bed, and the maximum effluent concentration is reduced.

It is also observed from Figure 14 that both leading and tailing transfer zones are a proportionate pattern type. Kumar and

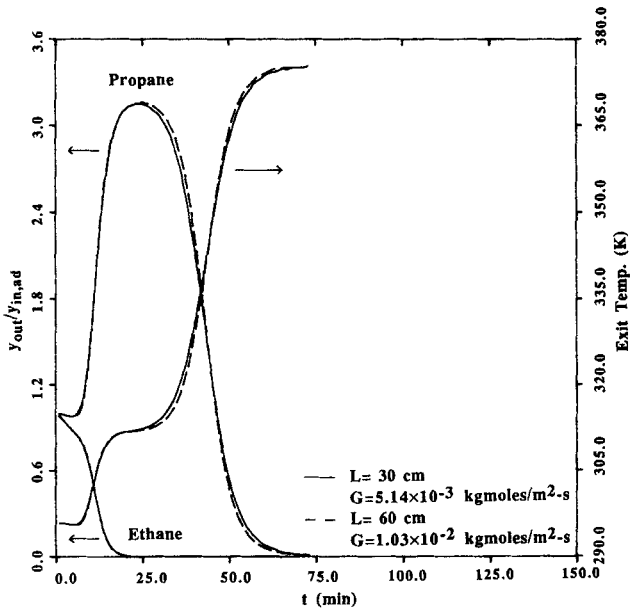

Figure 13. Effect of gas velocity on depletion curves at constant contact time (based on simulations): adiabatic case.

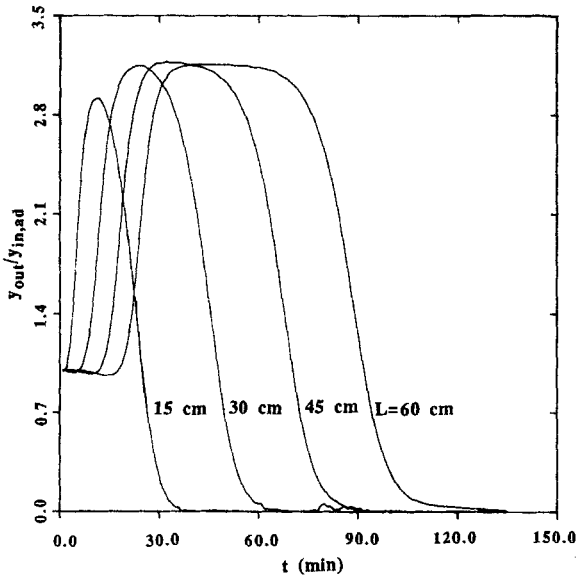

Figure 14. Propagation of the propane transfer fronts through a 60-cm adiabatic bed at regeneration step (based on simulations).

Dissinger (1986) and Schork (1986) also reported proportionate pattern transfer zones for hot purge regeneration of an adiabatic single-solute adsorber. As expected from equilibrium theory, the leading front travels much faster than the trailing front (Basmadjian et al., 1975a). The length of the concentration plateau region thus increases with the bed height.

Regeneration temperature

The effect of regeneration temperature is shown in Figure 15. Although the parameters of regeneration temperature and pressure are different between Runs DE-3 and DE-12, the effect of the former is much more prominent.

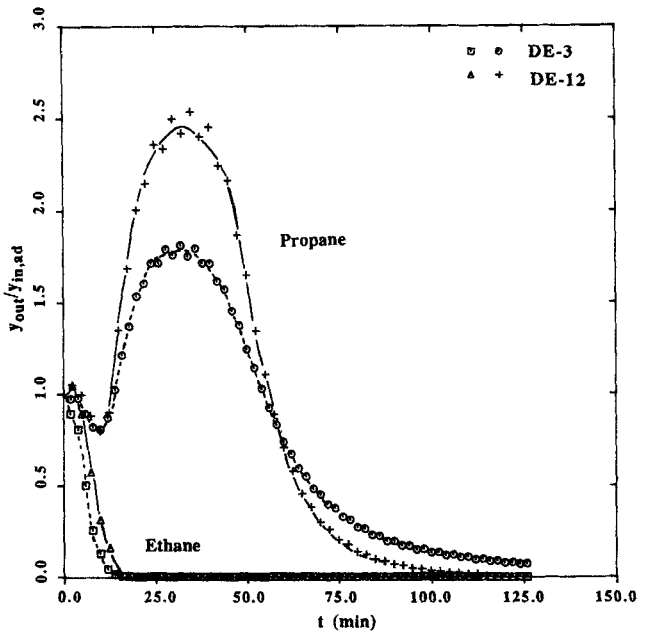

Figure 15. Effect of regeneration temperature on depletion curves.
Runs DE-3 (T_{Reg} = 344.1 K)
DE-12 (T_{Reg} = 380.4 K)

As mentioned earlier, for only a small amount of ethane in the bed there is little influence of regeneration temperature on the depletion curve of ethane. For propane, however, the situation is quite different. A higher regeneration temperature resulted in a higher roll-up level and a shorter desorption time. This effect is consistent with results reported by Schork (1986). Since the mass flow rates for these two runs were the same, the times of the propane concentration peaks coincided.

Analyzing the regeneration of a single-solute adsorber based on equilibrium theory, Basmadjian et al. (1975a) defined an important temperature and called it the "characteristic temperature." This is defined as the temperature at which the slope of the isotherm, evaluated at zero concentration, is equal to the ratio of heat capacity of adsorbent to that of carrier gas.

$$\left.\frac{dW}{dy}\right|_{y=0} = \frac{c_{ps}}{c_{pg}} \tag{6}$$

Above the characteristic temperature, the rear mass transfer zone will be at least partially a shock (Basmadjian et al., 1975a). The characteristic temperatures of the related single-component system in the present study are listed in Table 3.

Figure 16 shows the effect of regeneration temperature on the propane and ethane depletion curves. The results are based on numerical analysis of a 0.61-m-long adiabatic bed. The operating conditions are based on Run DE-22, except for the regeneration temperature. The regeneration temperatures are chosen in the range that embraces the characteristic temperature. The purge gas for all runs is hot nitrogen. As the regeneration temperature is increased, the rear fronts of concentration and temperature get sharper and the total regeneration time is decreased. The height of propane roll-up is also increased as regeneration temperature increases; this is to be expected, since the bed heats up faster at higher regeneration temperatures. As known from the isotherm, the higher the temperature of the adsorbent, the smaller the amount of adsorption. This result is the same as predicted by equilibrium theory. Kumar and Dissinger (1986) reported a similar effect of the regeneration temperature on the depletion curves of a single-adsorbate system.

As mentioned earlier, only a small amount of ethane remained in the bed at the beginning of the regeneration step. It can be seen from Figure 16b, however, that roll-up also occurs on the depletion of ethane, since the regeneration temperature is higher than the characteristc temperature of propane. This implies that a high purity of the key component could be

Table 3. Characteristic Temperatures for Various Systems at Different Pressures

Adsorbent	Adsorbate	Carrier Gas	Pres. kPa	Charact. Temp., K
Activated Carbon	Propane	Nitrogen	170	401
			239	414
		Helium	170	390
			239	401
Activated Carbon	Ethane	Nitrogen	170	335
			239	344
		Helium	170	325
			239	334

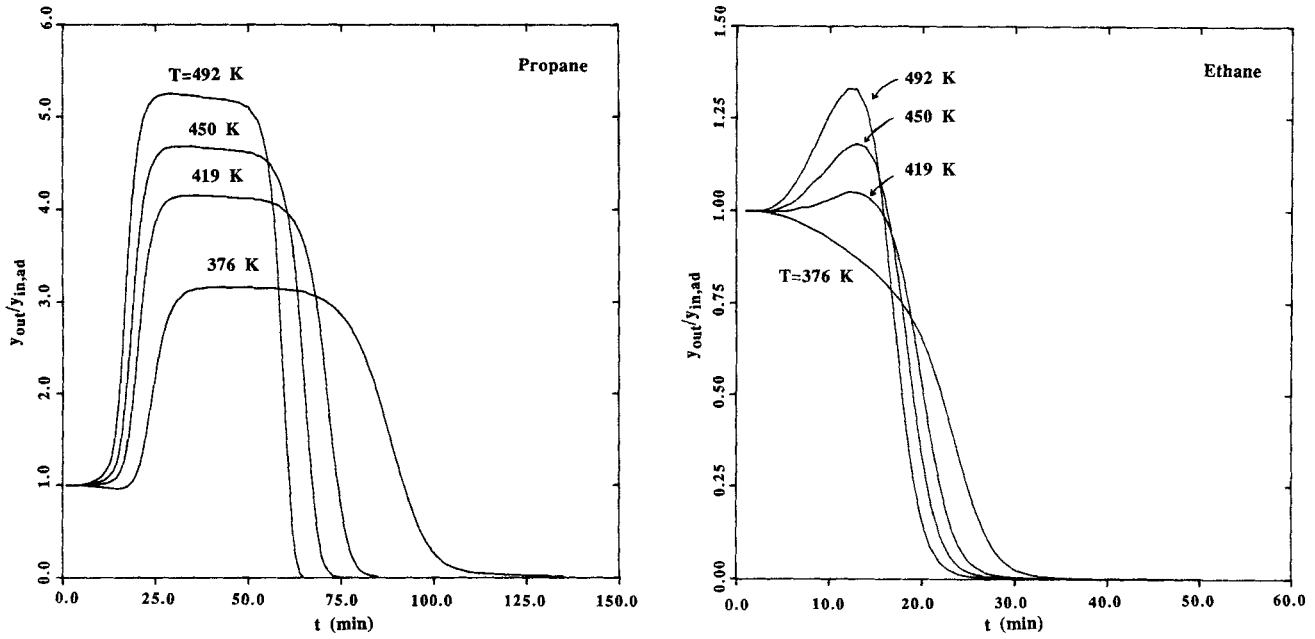

Figure 16. Effect of regeneration temperature on depletion curves for a 61-cm adiabatic bed (based on simulations).

obtained from the regeneration step, through the use of higher regeneration temperatures.

The specific purge gas and energy requirements are plotted vs. the regeneration temperature in Figure 17. The purge gas requirement decreases as the regeneration temperature is increased. This decrease is significant when regeneration temperature is lower than the characteristic temperature; however, the requirement decreases slowly as the regeneration temperature is further increased. The quantity of purge gas required finally decreases to the asymptotic value of c_{ps}/c_{pg}, the theoretical minimum purge requirement as the regeneration temperature approaches an infinitely high value. As Eq. 5 shows, the energy requirement is a function of both purge gas requirements, and the difference between regeneration and reference temperatures. Thus, there may exist an optimum regeneration temperature at which the energy requirement is minimum. From Figure 17, the minimum energy requirement is found to be around 394 K, which is slightly below the characteristic temperature of the key component. Kumar and Dissinger (1986) found the minimum requirement to be located at the characteristic temperature for a single-adsorbate system. Accordingly, one may conclude that a regeneration temperature in the vicinity of the characteristic temperature of the key component minimizes the energy requirement for thermal swing desorption of either single- or multisolute systems.

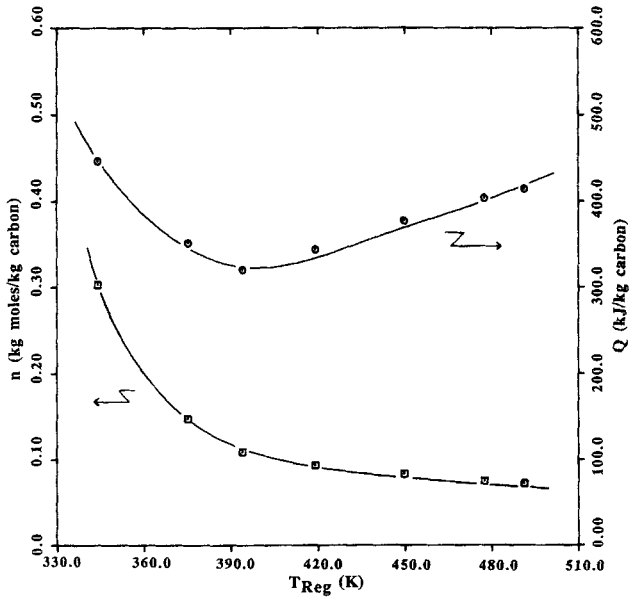

Figure 17. Effect of regeneration temperature on specific purge gas and energy requirement for a 61-cm adiabatic bed (based on simulations).

Initial bed loading

The effect of initial bed loading is shown in Figure 18. Runs DE-21 and DE-22 were operated under approximately the same conditions, except for the initial bed loading. The adsorption run previous to DE-21 was halted at the first detection of propane breakthrough, but Run DE-22 was not started until complete breakthrough of propane occurred. It is clear that the total regeneration times of these two runs were almost identical, even though the peak heights of depletion curves are different. One can deduce that the total regeneration time is relatively insensitive to initial bed loading levels. The same result was obtained experimentally by Basmadjian et al. (1975a) and Schork (1986) for the single-solute case.

These experimental results have indicated the insensitivity of regeneration time to the degree of saturation. The initial bed loading influence on the depletion curves can also be theoretically studied by varying feed compositions during the adsorption step. The total regeneration time is about the same, despite the differences in initial bed loading. A similar result was reported by Schork (1986) for single-solute adsorber regeneration and by Basmadjian et al. (1975a), based on equilibrium theory.

The insensitivity of regeneration time to level of loading indicates that the required regeneration time will not be affected by

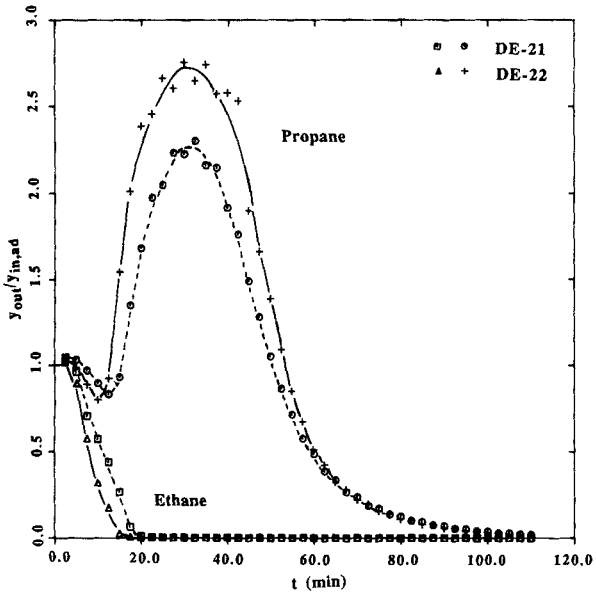

Figure 18. Effect of initial bed loading on depletion curves.
Runs DE-21 (partially saturated)
DE-22 (fully saturated)

fluctuations in the feed concentration during the adsorption step. The regeneration time required for a multisolute adsorber can be estimated from the regeneration time for an adsorber with only a single adsorbate.

Bed pressure

The effect of pressure on the depletion curves is presented in Figure 19. The total system pressures were 170 kPa and 239 kPa. The depletion curves shift to the right as system pressure increases indicating that total regeneration time is longer at higher pressure, even though the roll-up value is higher. This is because the driving force decreases when the system pressure is increased. As mentioned earlier, the regeneration temperature effect is more important than the pressure effect on desorption. When the regeneration temperature is above a certain value, high pressure operation is more efficient (see Figure 15). This result was also found by Basmadjian et al. (1975b).

Cyclic Process

Thermal swing adsorption is one of the oldest cyclic adsorber processes including adsorption and regeneration steps. Regeneration can be by hot or cold inert gas purge. Experimental and theoretical results on the TSA process are limited to the first cycle of adsorption, followed by regeneration using hot purge. Very little cyclic results on the TSA have been reported. Schork (1986) reported that the bed is rather clean after regeneration by a hot, inert purge. This implies that the cyclic steady state is approached in the second cycle. This is in contrast with cold, inert purge cycles, where several cycles are needed to approach a cyclic steady state (Bunke and Gelbin, 1978). In the present study, a hot, inert purge was used and the bed was found to be essentially clean after regeneration.

Since the isotherms are generally unfavorable for desorption, the cold purge is relatively ineffective. The length of time required for the regeneration step is thus always longer than that for the adsorption step. However, the dual-bed system, the most commonly used TSA cycle, requires time for adsorption and regeneration to be equal in length. A third bed, which increases the investment cost, may be needed to maintain equivalent continuous operations. For hot inert purge regeneration, the cooling step is traditionally followed. It was found in the present work that the cooling step could be omitted.

Ethane breakthrough curves with different initial conditions are illustrated in Figure 20. The adsorption step is stopped

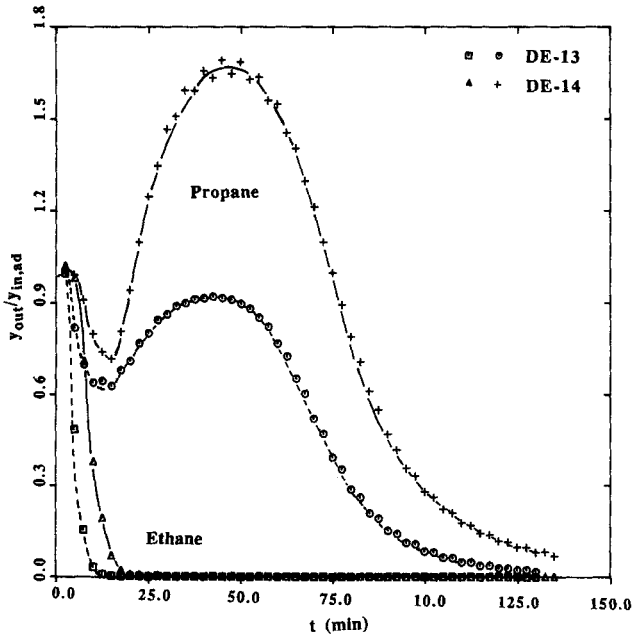

Figure 19. Effect of pressure on depletion curves.
Runs DE-13 (P = 170 kPa) and DE-14 (P = 239 kPa)

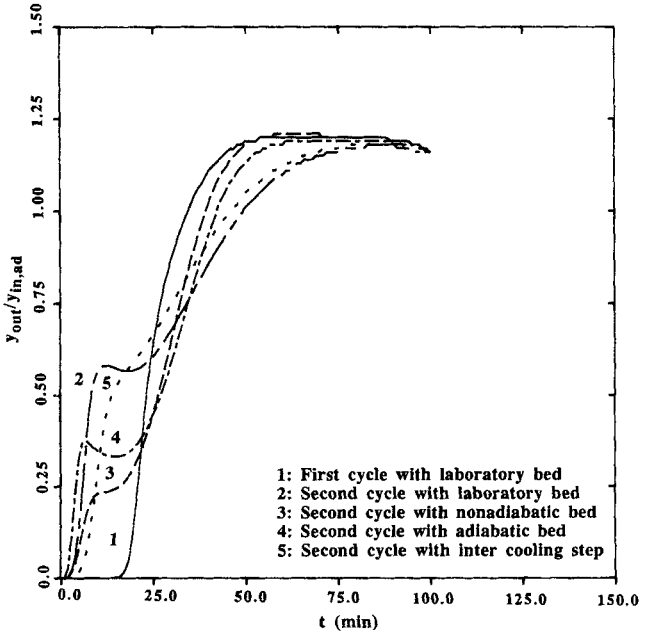

Figure 20. Ethane breakthrough curves with different initial conditions (based on simulation).

whenever the propane effluent concentration reaches 0.05%. The regeneration step is stopped whenever the propane effluent concentration is down to 0.05%. Curve 1 is a simulation of the first cycle adsorption in a laboratory scale bed, where the bed is initially cold. The remaining curves represent the simulation of the second cycle adsorption with a hot bed. Curve 5 is the case with five minutes cold inert purge (inter cooling step) after complete regeneration. The ethane breaks through the bed much earlier for the second cycle, since the bed is hot. The shapes of the second cycle breakthrough curves are completely different from those of the first cycle. This is to be expected, because the mass transfer is temperature-controlled in the hot bed. A readsorption occurs as the bed temperature cools down to a certain level, with corresponding increase in bed capacity. This broadens the mass transfer fronts. A process with a short, intercooling step can improve but little the mass transfer front and make it sharper. For the separation objective, however, such an improvement is not helpful.

Without the intercooling step, a TSA process can be operated continuously, by using a dual bed with hot purge regeneration. The regeneration temperature is selected around the characteristic temperature of the key component. The regeneration time can be adjusted to equal that of the adsorption step, by varying the superficial velocity of the purge gas.

Conclusions

Based on the analysis of the experimental and modeling results, the following conclusions are drawn:

- The mass transfer fronts of both breakthrough and depletion curves are of a proportionate pattern. The mass transfer zones are dispersive and elongating.
- The effluent concentration of the nonkey (less easily adsorbed) component generally overshoots its inlet concentration because of the displacement of the key (more easily adsorbed) component. The height of this "roll-up" is increased with the inlet concentration of the key component.
- The breakthrough curve of the key component is little affected by the presence of a nonkey component, when both have low concentration in the feed.
- Nitrogen is competitive with ethane for adsorption on activated carbon, when the nitrogen/ethane ratio in the feed is high.
- For the separation of ethane and propane by adsorption, a higher system pressure is favorable. A high system pressure, however, is unfavorable for hot purge regeneration.
- The bed efficiency for the adsorptive separation of a gas mixture improves with increasing contact time (decreasing superficial velocity at a given fixed-bed height).
- The time to regenerate a fixed bed is controlled by the desorption of the key component and changes very little when that same component is the only adsorbate.
- Purge gases with higher heat capacities (e.g., nitrogen) result in shorter regeneration times and smaller amounts of purge gas required.
- Regeneration time and energy requirements are minor functions of the level of the initial bed loading. This is true for both adiabatic and nonadiabatic systems.
- A minimum in the regeneration energy requirement vs. temperature curve occurs at a temperature slightly below the characteristic temperature of the key component.
- The cooling step following hot purge regeneration can be omitted if the key component meets the criteria proposed by Basmadjian (1975).

Notation

a_p = geometric surface area, m^{-1}
c_{pg} = heat capacity of the carrier gas, J/kmol · K
c_{ps} = heat capacity of the adsorbent, J/kg · K
G = superficial molar gas flow rate, kmol/m^2 · s
ΔH = heat of adsorption, J/kmol
L = bed length, m
n = specific regenerant requirement, kmol/kmol adsorbent
Q = specific energy requirement, J/kg adsorbent
$t_{1\%}$ = complete regeneration time, min
T_O = reference temperature, K
T_F = feed temperature, K
T_p = plateau temperature, defined as Eq. 3, K
T_{reg} = regenerant temperature, K
W_F, W_p = solid-phase concentration based on feed and plateau temperature kmol/kg solid
y_F = mole ratio of gaseous adsorbate to carrier gas

Greek letters

ϵ_{ex} = external bed void volume, fractional
ϵ_p = particle porosity, fractional
ρ_b = bulk density, kg/m^3

Literature Cited

Basmadjian, D., "On the Possibility of Omitting the Cooling Step in Thermal Gas Adsorption Cycles," *Can. J. Chem. Eng.*, **53**, 234 (1975).

Basmadjian, D., K. D. Ha, and C-Y. Pan, "Nonisothermal Desorption by Gas Purge of Single Solution in Fixed-Bed Adsorbers: I. Equilibrium Theory," *Ind. Eng. Chem. Process Des. Dev.*, **14**(3), 328 (1975a).

———, "Nonisothermal Desorption by Gas Purge of Single Solution in Fixed-Bed Adsorbers: II. Experimental Verification of Equilibrium Theory." *Ind. Eng. Chem. Process Des. Dev.*, **14**(3), 340 (1975b).

Bunke, G., and D. Gelbin, "Breakthrough Curves in the Cyclic Steady State for Adsorption Systems with Concave Isotherms," *Chem. Eng. Sci.*, **33**, 101 (1978).

Cochran, T. W., R. L. Kabel, and R. P. Danner, "Vacancy Solution Theory of Adsorption Using Flory-Huggins Activity Coefficient Equations," *AIChE J.*, **31**(2), 268 (1985).

Gariepy, R. L., and I. Zwiebel, "Adsorption of Binary Mixtures in Fixed Beds," *AIChE Symp. Ser.*, **67**(117), 17 (1971).

Huang, C-C., "Thermal Regeneration of Fixed Multicomponent Adsorption Beds" PhD Diss., Univ. of Texas, Austin (1987).

Huang, C.-C., and J. R. Fair, "Study of Adsorption and Desorption of Multiadsorbates in a Fixed Bed," *AIChE J.*, **34**, 1861 (1988).

Kumar, R., and G. R. Dissinger, "Non-Equilibrium, Non-Isothermal Desorption of Single Adsorbate by Purge," *Ind. Eng. Chem. Process Des. Dev.*, **25**, 456 (1986).

Madey, R., P. J. Photinos, D. Rothstein, D. R. J. Forsythe, and J.-C. Huang, "Adsorption Interference in Mixtures of Adsorbate Gases Flowing through Activated Carbon Adsorber Beds," *Langmuir*, **2**, 173 (1986).

Schork, J. M., "Thermal Regeneration of Fixed Adsorption Beds," PhD Diss., Univ. of Texas, Austin (1986).

Schork, J. M., and J. R. Fair, "Parametric Analysis of Thermal Regeneration of Adsorption Beds," *Ind. Eng. Chem. Res.*, **27**(3), 457 (1988).

Manuscript received Dec. 2, 1987, and revision received July 14, 1989.